Correlation between Cirrus Particle Optical Properties: Microphysics and Implications for Spaceborne Remote Sensing

J. Reichardt[1,2], M. Hess[3], S. Reichardt[1,2], A. Behrendt[4], T. J. McGee[2]

1. Joint Center for Earth Systems Technology, University of Maryland Baltimore County, Baltimore, MD
2. Atmospheric Chemistry and Dynamics Branch, Laboratory for Atmospheres, NASA Goddard Space Flight Center, Greenbelt, MD
3. Deutsches Fernerkundungsdatenzentrum, Deutsches Zentrum für Luft- und Raumfahrt Oberpfaffenhofen, Weßling, Germany
4. Radio Science Center for Space and Atmosphere, Kyoto University, Uji, Kyoto, Japan

Submitted to

Science

Corresponding author address: Dr. Jens Reichardt, Code 916, NASA Goddard Space Flight Center, Greenbelt, MD 20771; Phone: 301-614-5989; Fax: 301-614-5903; Email: reichardt@code916.gsfc.nasa.gov.

Cirrus clouds are widely recognized as a major component of the energy budget of the Earth-atmosphere system (*1*), yet the magnitude of cirrus climate forcing remains highly uncertain, despite considerable efforts to quantify it (*2*, *3*). The difficulties stem primarily from the fact that the radiative forcing of cirrus clouds, which are predominantly comprised of ice particles, is crucially dependent on the particle shapes, sizes and number concentration. An accurate assessment of cirrus cloud forcing poses a major challenge because it essentially requires a global climatology of cirrus clouds that includes microphysical properties.

There is no measurement system to date that can provide both global statistics and microphysical information. Satellite-borne sounders provide global coverage, but active spaceborne remote sensing techniques are limited in the number of cloud quantities directly measurable, and passive instruments have difficulties in retrieving basic parameters such as cloud vertical structure, and in the detection of thin cirrus. On the other hand, ground-based remote systems such as light radar (lidar) can provide high resolution and simultaneous measurements of multiple cloud and atmospheric parameters, but with limited coverage. Thus, ground-based lidar and satellite measurements provide complementary information, and the question we explore here is whether, and how, the knowledge gained from lidar measurements can be used to enhance the retrieval of satellite data to provide a global, statistical estimate of cirrus cloud radiative forcing.

Abstract

Cirrus measurements obtained with a ground-based polarization Raman lidar at 67.9°N in arctic winter reveal a strong correlation between the particle optical properties, specifically depolarization ratio and extinction-to-backscatter ratio, for ambient cloud temperatures above ~ -45°C, and an anti-correlation for colder temperatures. Similar correlations are evident in a 2-year midlatitude (53.4°N) cirrus data set. Scattering calculations show that the observed dependences can be interpreted in terms of the shapes and sizes of the cirrus ice particles. These findings suggest a retrieval method for determining cirrus extinction profiles from spaceborne lidar polarization data.

Three independent cloud optical parameters can be measured with lidar: the extinction coefficient, the backscatter coefficient, and the depolarization ratio δ (ratio of elastic backscatter signals with polarization planes orthogonal and parallel, respectively, to the linearly polarized lidar radiation source). The extinction-to-backscatter (lidar) ratio S and the depolarization ratio do not depend on the particle number density, and therefore contain range-resolved information about the scattering properties of the cloud particles. Simultaneous measurements of lidar and depolarization ratios have been obtained with high spectral resolution lidars (*4*) and polarization Raman lidars (*5*), but correlations between these optical properties and their relation to particle microphysical properties have not yet been investigated.

Figure 1 provides an overview of three cirrus cloud systems measured with the polarization Raman lidar of the GKSS Research Center Geesthacht (*5*) above the Swedish research facility Esrange (67.9°N) in January 1997. These cases have been selected from cirrus observations on 14 of the 26 days the lidar was operated for outstanding data quality and duration of the sightings. The evolution of the geometrical structure and δ vary strongly from case to case. To study the scattering behavior of the cirrus particles (*6*), height profiles of S and δ have been determined for three independent observation periods during each cirrus event (*7–9*). Figure 2 is a plot of δ versus S for all cirrus altitudes of these 9 measurement segments (A1–A3, B1–B3, and C1–C3). The data show two distinct linear correlation patterns.

δ and S are negatively correlated when the depolarization ratio is high, and they are positively correlated when the depolarization ratio is low. The groups merge at $S \sim 22\,\mathrm{sr}$ with δ values around 40% (*10*). The data points of individual measurement segments, e. g., B2, are not scattered over both subsets of data, but are confined to a relatively small section of one of the correlation lines. The correlations strongly suggest that the cirrus observations can be given a microphysical interpretation, because S and δ are determined by the scattering phase matrix of the cirrus particle ensemble which in turn depends on the size and shape of the crystals. We investigate this hypothesis below by examining the dependence of the particle properties on ambient cloud temperature T_C and also by comparison with calculations.

Temperature is the principal factor that governs the crystal shape (*11*), and so the observed systematic variation of lidar and depolarization ratios should depend on T_C. For this purpose T_C values that are associated with the particle optical properties of each data subset have been calculated from radiosonde measurements. The results of the analysis are presented in Fig. 3. T_C is indeed tightly connected to the optical properties, with T_C being coldest for cirrus clouds that are characterized by low S and high δ, whereas T_C is warmest for low S and low δ. Above $S \sim 22\,\mathrm{sr}$ cloud temperatures of high-δ and low-δ data groups are not distinguishable.

Secondly, the observed S and δ values have been compared with theoretical particle optical properties. Because $T_\mathrm{C} < -40^\circ\mathrm{C}$ for the overwhelming

majority of the data, the existence of water droplets can be excluded (*12*), and it is assumed that the cirrus clouds consist solely of solid ice particles. Figure 2 shows the results of calculations for crystals that have a basically column-like or plate-like hexagonal shape (*13*). In general, theoretical and observed optical properties agree well. Column and plate δ values match the values of the high-δ (cold T_C) and low-δ (warm T_C) data subsets, particularly for small S. For larger S, the computed optical properties mark the boundaries of the measurements. This, and the fact that the absolute values of the slopes of the two regression lines are almost identical, imply that the observed cirrus clouds consist of mixtures of column- and plate-like particles. In natural ice clouds length and aspect ratio (length divided by width) of the ice crystals are correlated (*14*); small crystals tend to have aspect ratios close to one, whereas large columns and plates have aspect ratios $\gg 1$ and $\ll 1$, respectively. Applying this correlation to the data in Fig. 2, we find that the sizes of the scattering cirrus crystals increase with increasing S. This, however, does not necessarily mean that the ice particles (*6*) are larger for large S than for small S: A morphologically complex or composite particle, such as an aggregate of crystals of simple spatial symmetry, has been shown to scatter similarly to the ensemble of basic crystals that formed it (*15*). So a small ice particle consisting of one or more relatively large ice crystals may still have a higher S value than a large ice particle formed from relatively small crystals.

In summary, we propose the following microphysical interpretation of the observations. In the coldest regions of the clouds, ice particles with aspect ratios ~ 1 form. For increasing T_C, the ice particles get larger and consist of a mixture of column-like and plate-like crystals, but remain predominantly column-like. Around $T_C = -45°C$, the dominant fundamental shape of the crystals gradually shifts from columns to plates. At even warmer temperatures in the lower regions of the cirrus clouds, particle size and morphological complexity increase with T_C. The high correlation of the low-δ data subset may be due to the fact that hexagonal plates and complex crystals such as hollow columns, bullet rosettes, and aggregates have almost the same scattering signature, if rough crystal surfaces are assumed (*16, 17*). This microphysical interpretation combines in a consistent manner the observed cirrus optical properties and temperature data with theoretical studies (*15, 16*), laboratory experiments of ice particle growth (*18, 19*), *in situ* particle sampling (*19, 20*), and remote measurements of cirrus clouds at other locations (*21, 22*).

The previously discussed correlations between the particle optical properties of Arctic cirrus clouds, specifically δ and S, are an important finding on their own, as they have proven to be useful for the interpretation of the cirrus data measured over Esrange and for defining constraints to ray-tracing calculations of particle scattering for remote sensing applications (*13*). However, the question arises as to whether these same correlations are

characteristic of cirrus clouds in general (*23*). A shortcoming of the Esrange measurements is the lack of information about supersaturation, after T_C the second principal atmospheric parameter controlling particle growth (*11*). Because the tropospheric absolute humidity was low as confirmed by lidar water-vapor measurements (*17*), the supersaturation and particle growth rates were probably low also, and the results may not apply to ice particles that formed rapidly such as those found in glaciated outflows of convective clouds.

As a first check for the generality of the findings, measurements taken with the GKSS Raman lidar (*5*) at its home base at Geesthacht, Germany (53.4°N), between 1994 and 1996 have been analyzed for cirrus cloud properties. As compared to the cirrus clouds measured over Esrange, the observed cirrus clouds over Geesthacht were optically thinner and appeared at higher altitudes. Furthermore, atmospheric conditions at Geesthacht were often not favorable for lidar measurements. Therefore only cloud-mean values of S and δ can be determined for each cirrus event. The results are shown in Fig. 4. It is evident that δ and S of the northern midlatitude cirrus clouds are correlated as well, and that the functional dependence of δ on S is the same as for the low-δ data group of the Arctic cirrus clouds. The almost complete lack of midlatitude cirrus data with $\delta > 40\%$, even for very cold ambient temperatures, suggests differences between the growth conditions of the ice particles at the two sites.

These promising results should encourage further efforts to even better understand the relation between optical and microphysical cirrus properties and cirrus-particle formation, and to define the atmospheric conditions under which the correlations between depolarization and lidar ratio hold. This knowledge would have important implications for generation of an advanced global cirrus climatology which would then include information about the particle extinction coefficient, one of the most important cloud parameters necessary for radiative-transfer calculations in climate studies. For experimental reasons this quantity cannot be measured directly with spaceborne lidars, but the work presented here suggests an indirect method. If an elastic depolarization lidar was deployed on a satellite and if the δ versus S correlations were applicable, the depolarization measurement could be used to derive an estimate of the height-dependent cirrus lidar ratio which in turn would allow to solve the elastic-backscatter lidar equation for the particle extinction coefficient (*24*).

Figure Captions

Fig. 1. Height versus time display of depolarization ratio generated from consecutive lidar profiles of cirrus clouds measured over northern Sweden. From each cirrus observation three measurement periods (arrows) have been chosen for further data analysis. The measurement wavelength is 355 nm.

Fig. 2. Depolarization ratio versus lidar ratio scatter plot of the cirrus measurements A1–3, B1–3, C1–3 shown in Fig. 1 (●). The distribution of the data points is bifurcated, δ and S of the two obvious data subsets with high δ (○) and low δ (○) are strongly correlated (regression lines and coefficients in corresponding colors). Calculated δ-versus-S values of hexagonal columns (▼) and hexagonal plates (▲) suggest that, for small S, cirrus scattering is predominantly by column-like or plate-like particles, whereas for larger S scattering contributions of both particle types seem to mix. Aspect ratios of columns (1.4, 1.3, 1.5, 2.5, 3.8, 5.9, from left to right) and plates (0.3, 0.2, 0.13, 0.08, 0.05, 0.04, from left to right) indicate an increase in crystal size with increasing lidar ratio (*6*).

Fig. 3. Cloud temperatures of the data subsets with low (red) and high depolarization ratios (blue, cf. Fig. 2) averaged over 2.5-sr S bins. Error bars indicate statistical uncertainties of the temperature means. Temperature profiles are taken from quasi-simultaneous radiosonde ascents at the lidar site or at the near-by radiosonde station Luleå.

Fig. 4. Depolarization ratio versus lidar ratio scatter plot of cirrus clouds measured over Geesthacht, northern Germany (53.4°N). Data represent cloud-layer mean values of cirrus events on different days. Regression lines of Fig. 2 are shown for comparison.

References and Notes

1. K. N. Liou, *Mon. Weather Rev.* **114**, 1167 (1986).
2. G. L. Stephens, S. Tsay, P. W. Stackhouse, Jr., P. J. Flatau, *J. Atmos. Sci.* **47**, 1742 (1990).
3. M. B. Baker, *Science* **276**, 1072 (1997).
4. E. W. Eloranta, P. Piironen, in *Advances in Atmospheric Remote Sensing with Lidar*, A. Ansmann, R. Neuber, P. Rairoux, U. Wandinger, Eds. (Springer-Verlag, New York, 1997), pp. 83–86.
5. J. Reichardt, U. Wandinger, M. Serwazi, C. Weitkamp, *Opt. Eng.* **35**, 1457 (1996).
6. Cirrus scatterers formed from frozen water are generally referred to as ice particles here. An ice particle can be a single ice crystal with simple spatial symmetry, or a morphologically complex aggregate of ice crystals.
7. S profiles are corrected for multiple scattering. Correction factors are calculated with a radiative-transfer model that takes into account light scattering by molecules, aerosols and cirrus cloud in the whole atmospheric column sensed (*25*, *26*). Following visual observations of boundary-layer ice haze, ice particles with 1–20 μm particle diameters and an extinction coefficient of 0.2 km^{-1} are assumed below 2 km height. Cirrus clouds are assumed to consist of 10–80 μm hexagonal crystals of slightly distorted symmetry in random orientation. Scattering by boundary-layer ice aerosol affects correction factors for altitudes $<\sim$ 5 km only.

8. In optically thin cirrus and at cloud boundaries δ has to be corrected for the influence of molecular scattering as it tends to depress the measured δ values. E.g., for a true δ value of 30%, a depolarization by molecular scattering of 0.7% and a ratio of particle to molecule backscatter coefficient of 2.5, the measured δ value is 20%.

9. A multiple-scattering correction of the depolarization ratio is not necessary, as the measurements showed no apparent increase in molecular depolarization above the cirrus clouds which would occur in the presence of depolarizing cloud multiple small-angle forward scattering. Generally, ground-based narrow-field-of-view lidar measurements of δ that are affected by multiple scattering are a rare phenomenon in high-altitude ice clouds (*27*).

10. The data set was also carefully examined for dependences of S and δ on distance Δz of the particles from the cloud top to investigate the effect of particle sedimentation. However, the absolute values of the correlation coefficients given in Fig. 2 are significantly larger than those found for S or δ as functions of Δz (between 0.2 and 0.35).

11. In laboratory experiments it has been shown that the air temperature determines whether the ice particles grow to basically column-like or plate-like crystals, with columns generally found at colder temperatures. Instead, supersaturation controls the growth rate and the morphological complexity of the crystal; secondary growth features like dendritic crystal branches develop only when the air is supersaturated relative to

liquid water (*28*).

12. A small cloud droplet of pure water can remain in a supercooled state until its temperature approaches the temperature of homogeneous freezing near −39°C (*29*). Heterogeneous nucleation initiated by ice nuclei that are usually present in the atmosphere occurs at much warmer temperatures. The coldest temperatures at which liquid droplets have been reported to exist in cirrus and convective clouds are −36°C and −37.5°C, respectively (*30*, *31*). Liquid droplets of aqueous acids can exist at atmospheric temperatures < −39°C. Freezing point depression resulting from an influx of stratospheric volcanic aerosols into the cirrus-generating regions has been used to explain the observation of short-lived cloud cells of liquid drops in cirrus clouds at −49°C (*32*). However, this rare phenomenon can be excluded from the discussion here, because at the time of the measurements the aerosol content of the lower stratosphere was very low.

13. Atmospheric crystals rarely have perfect hexagonal shape, but exhibit distortions such as ice core inhomogeneities and angles between crystal faces that deviate from the theoretical values. In our ray-tracing calculations these irregularities are accounted for by statistical roughening of the crystal surfaces (*33*). Surface roughness is assumed to be the same for columns or plates of all aspect ratios, and is chosen so that the calculated δ and S values both fall within the observation ranges of these quantities. Generally, an increase in surface roughness

leads to higher S and lower δ. One shortcoming of the ray-tracing approach is that physical-optics effects are not taken into account. For crystals with imperfections, however, this approximation may be sufficient, because crystal shape distortions tend to smooth the features of the scattering phase matrix elements at lateral and backward scattering angles. Random orientation of the cirrus particles is assumed as implied by the lidar data (the distinct optical scattering signature of horizontally aligned cloud particles, i.e., $S <\sim 5\,\mathrm{sr}$ and $\delta <\sim 5\%$, has not been observed during the whole campaign). To reduce statistical errors, scattering phase matrix elements calculated at 179- and 180-degree scattering angle are averaged.

14. A. H. Auer, Jr., D. L. Veal, *J. Atmos. Sci.* **27**, 919 (1970).

15. A. Macke, *Appl. Opt.* **32**, 2780 (1993).

16. P. Yang, K. N. Liou, *Contr. Atmos. Phys.* **71**, 223 (1998).

17. This interpretation assumes supersaturation relative to ice throughout the cirrus vertical extent. An alternative explanation for the low-δ data subset is sedimentation of plate-like particles into air masses that are not saturated relative to ice, with sublimation leading to decrease in size or alteration of shape. Information about supersaturation is therefore necessary to resolve the ambiguity of the particle optical properties. However, humidity data are not available for this campaign, although water vapor and cirrus clouds were measured simultaneously with the same lidar system (*5*). The water-vapor return signal rapidly

approached the detection limit above $\sim 3\,\mathrm{km}$, so that relative humidity could not be determined at cloud altitudes.

18. T. Gonda, T. Yamazaki, *J. Cryst. Growth* **45**, 66 (1978).

19. A. J. Heymsfield, *J. Atmos. Sci.* **30**, 1650 (1973).

20. A. J. Heymsfield, J. Iaquinta, *J. Atmos. Sci.* **57**, 916 (2000).

21. C. M. R. Platt, A. C. Dilley, *J. Atmos. Sci.* **38**, 1069 (1981).

22. J. Reichardt, *Phys. Chem. Earth (B)* **24**, 255 (1999).

23. Particle properties of the other cirrus measurements taken over Esrange in January 1997 fit well in the present classification scheme. One cirrus cloud, however, showed relatively low δ ($\sim 20\%$) and high S (20–27 sr) values which suggest that this cloud consisted of plate-like or complex crystals alone and that column-like scatterers were absent.

24. The effect of multiple scattering on depolarization measurements from space is negligible in cirrus clouds with moderate extinction coefficients (*34*).

25. J. Reichardt, M. Hess, A. Macke, *Appl. Opt.* **39**, 1895 (2000).

26. J. Reichardt, *Appl. Opt.* **39**, 6058 (2000).

27. U. Wandinger, A. Ansmann, C. Weitkamp, *Appl. Opt.* **33**, 5671 (1994).

28. B. J. Mason, G. W. Bryant, A. P. van den Heuvel, *Phil. Mag.* **8**, 505 (1963).

29. C. A. Jeffery, P. H. Austin, *J. Geophys. Res.* **102**, 25,269 (1997).

30. K. Sassen, K. N. Liou, S. Kinne, M. Griffin, *Science* **227**, 411 (1985).

31. D. Rosenfeld, W. L. Woodley, *Nature* **405**, 440 (2000).

32. K. Sassen, *Science* **257**, 516 (1992).

33. M. Hess, R. B. A. Koelemeijer, P. Stammes, *J. Quant. Spectrosc. Radiat. Transfer* **60**, 301 (1998).

34. Y. Hu *et al.*, *J. Quant. Spectrosc. Radiat. Transfer*, in press.

35. Part of this work was funded by the European Commission under grant ENV4-CT95-0162 and the German Bundesministerium für Bildung, Wissenschaft und Technologie, grant 01LO9504/5.

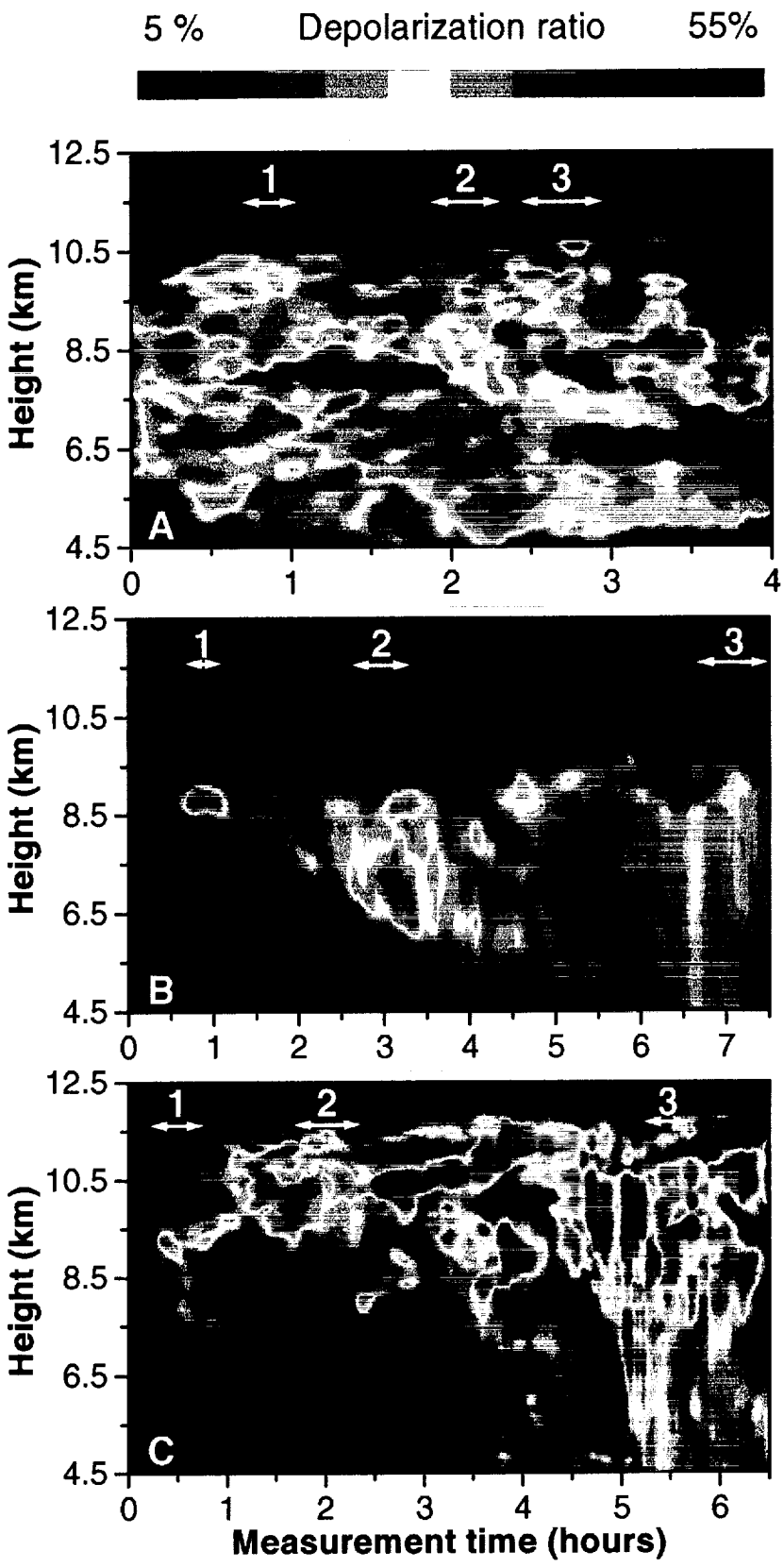

Fig. 1

J. Reichardt
Science

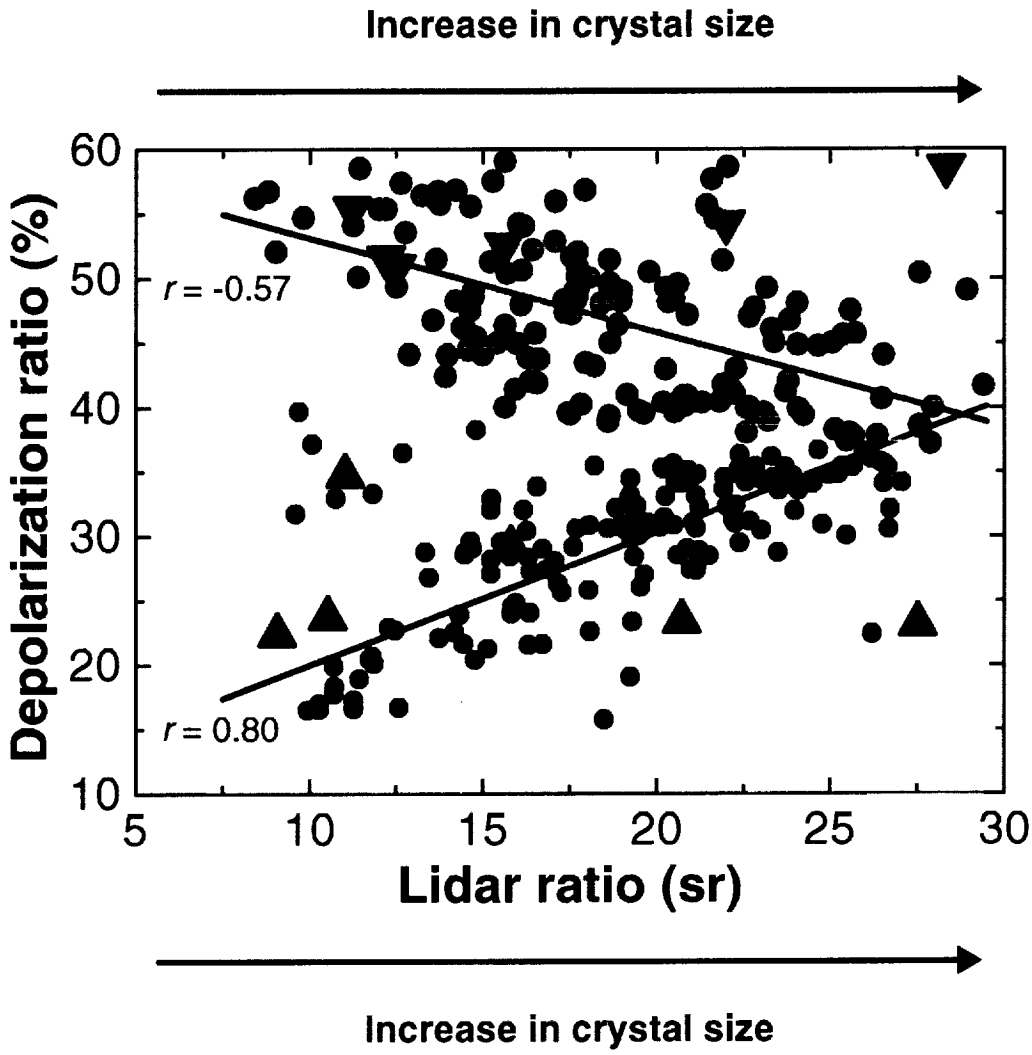

Fig. 2

J. Reichardt
Science

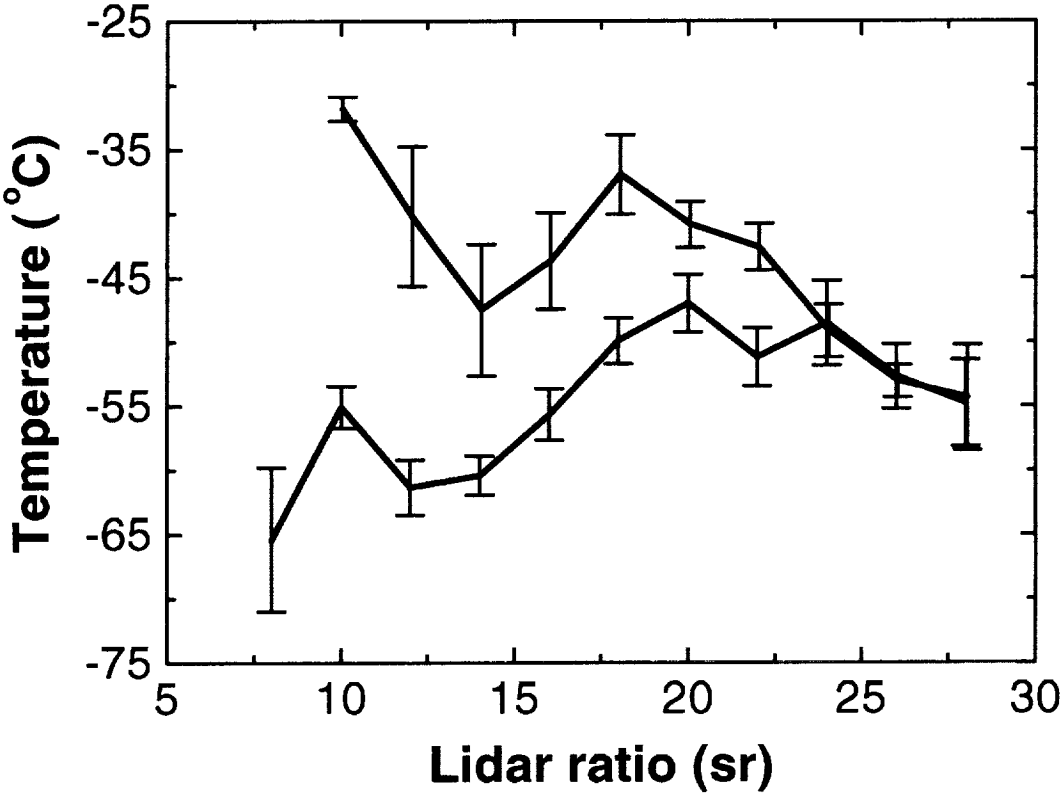

Fig. 3

J. Reichardt
Science

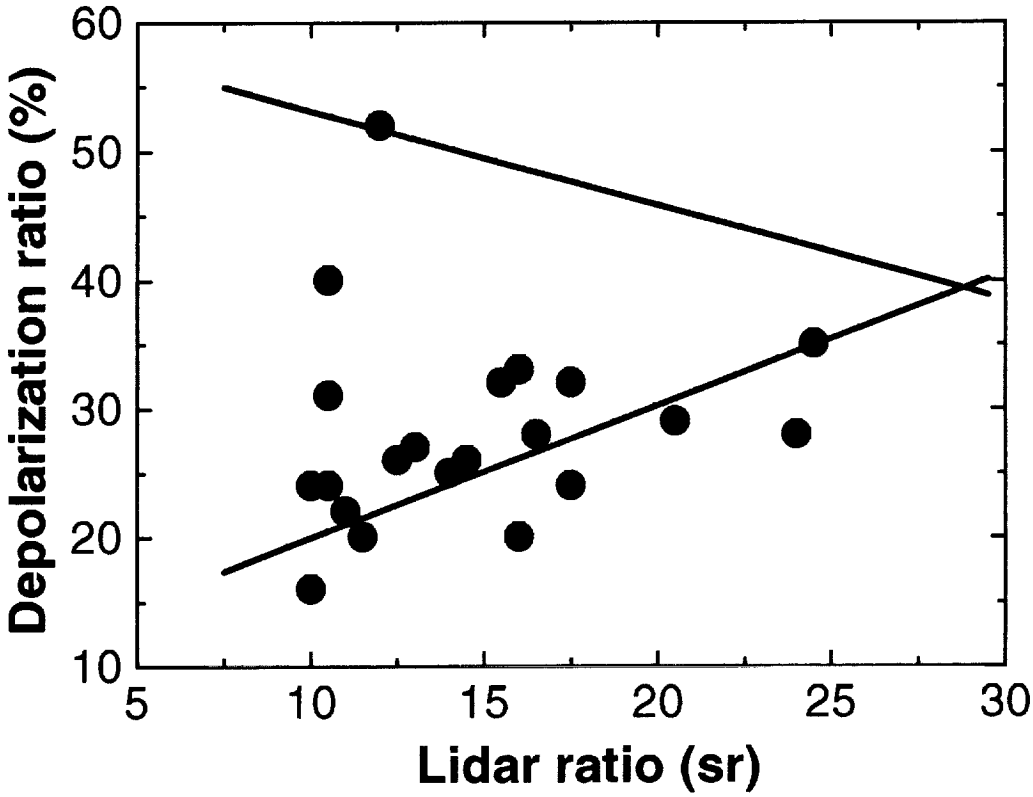

Fig. 4

J. Reichardt
Science

2001-04-24

POPULAR SUMMARY of "Correlation between Cirrus Particle Optical Properties: Microphysics and Implications for Spaceborne Remote Sensing"

-> Jens Reichardt (JCET), Susanne Reichardt (JCET), Thomas J. McGee
Atmospheric Chemistry and Dynamics Branch, Laboratory for Atmospheres, NASA Goddard Space Flight Center, Greenbelt, MD

-> Michael Hess
Deutsches Fernerkundungsdatenzentrum, Deutsches Zentrum für Luft- und Raumfahrt Oberpfaffenhofen, Weßling, Germany

-> Andreas Behrendt
Radio Science Center for Space and Atmosphere, Kyoto University, Uji, Kyoto, Japan

-> Submitted to Science

Cirrus measurements obtained with a ground-based polarization Raman lidar at 67.9°N in arctic winter reveal a strong correlation between the particle optical properties, specifically depolarization ratio and extinction-to-backscatter ratio, for ambient cloud temperatures above -45°C, and an anti-correlation for colder temperatures. Similar correlations are evident in a 2-year midlatitude (53.4°N) cirrus data set.
Scattering calculations show that the observed dependences can be related to the microphysical properties of the cirrus clouds, specifically to the shapes and sizes of the ice particles. This microphysical interpretation is consistent with current theoretical studies and laboratory experiments of ice particle growth, with *in situ* particle sampling, and with remote measurements of cirrus clouds at other locations.

This is the first time correlations between the optical parameters and a relation between the optical and microphysical properties of cirrus clouds have been reported. The implications of these results are important for atmospheric research: First, the correlations between the particle optical properties are useful for defining constraints to ray-tracing calculations of particle scattering for remote sensing applications. Second, the observations reveal a new method for determining the microphysical properties of cirrus clouds, which can then be used to infer the ratio of light transmitted and scattered back to space. This is not only important for similar instruments, such as spaceborne lidars which will fly over the next few years, but also for the understanding of the general cirrus cloud radiative transfer problem.